Muon spin rotation/relaxation measurements of the noncentrosymmetric superconductor Mg$_{10}$Ir$_{19}$B$_{16}$

A. A. Aczel,[1] T. J. Williams,[1] T. Goko,[1,2,3] J. P. Carlo,[3] W. Yu,[4] Y. J. Uemura,[3] T. Klimczuk,[5,6] J. D. Thompson,[5] R. J. Cava,[7] and G. M. Luke[1,8,9]

[1]*Department of Physics and Astronomy, McMaster University, Hamilton, Ontario, Canada L8S 4M1*
[2]*TRIUMF, 4004 Wesbrook Mall, Vancouver, British Columbia, Canada V6T 2A3*
[3]*Department of Physics, Columbia University, New York, New York 10027, USA*
[4]*Department of Physics, Renmin University of China, Beijing 100872, China*
[5]*Los Alamos National Laboratory, Los Alamos, New Mexico 87545, USA*
[6]*European Commission, Institute for Transuranium Elements, Joint Research Center, P.O. Box 2340, D-76125 Karlsruhe, Germany*
[7]*Department of Chemistry, Princeton University, Princeton, New Jersey 08544, USA*
[8]*Brockhouse Institute for Materials Research, McMaster University, Hamilton, Ontario, Canada L8S 4M1*
[9]*Canadian Institute of Advanced Research, Toronto, Ontario, Canada M5G 1Z8*

We have searched for time-reversal symmetry-breaking fields in the noncentrosymmetric superconductor Mg$_{10}$Ir$_{19}$B$_{16}$ via muon spin relaxation (μSR) in zero applied field. We also measured the temperature dependence of the superfluid density by muon spin rotation in transverse field to investigate the superconducting pairing symmetry in two polycrystalline samples of significantly different purities. In the high-purity sample, we detected no time-reversal symmetry-breaking fields greater than 0.05 G. The superfluid density was also found to be exponentially flat as $T \rightarrow 0$ and so can be fit to a single-gap BCS model. In contrast, the lower purity sample showed an increase in the zero-field μSR relaxation rate below T_c corresponding to a characteristic field strength of 0.6 G. While the temperature dependence of the superfluid density was also found to be consistent with a single-gap BCS model, the magnitude as $T \rightarrow 0$ was found to be much lower for a given applied field than in the case of the high-purity sample. These findings suggest that Mg$_{10}$Ir$_{19}$B$_{16}$ is a superconductor characterized by a single-gap function with no nodes and sample quality drastically affects the superconducting properties of this system.

The spin-singlet Cooper pairs of conventional superconductors require the corresponding superconducting order parameter to exhibit time-reversal symmetry.[1] For spin-triplet pairing, time-reversal symmetry is characteristic of only some of the possible superconducting states, but Anderson originally hypothesized that these should all have spatial inversion symmetry.[2] This then suggested that a material lacking an inversion center should be an unlikely candidate for spin-triplet pairing. However, a potential exception was found recently with the discovery of superconductivity in the noncentrosymmetric, heavy-fermion compound CePt$_3$Si,[3] where the upper critical field was found to exceed the paramagnetic limiting field in this material, suggesting possible spin-triplet pairing. A mixed spin-singlet and triplet pairing state was proposed to resolve this controversy, and this exotic possibility has stimulated significant effort in both theoretical and experimental studies to understand superconductors lacking inversion centers.

The proposed mixed pairing state was found to be a consequence of superconductivity in a material that exhibits spin-orbit coupling (SOC) but lacks inversion symmetry. In this case, the usually doubly degenerate electronic bands become nondegenerate almost everywhere in the Brillouin zone and the resulting superconducting states can no longer be classified according to parity. While noncentrosymmetric, heavy-fermion superconductors[3–6] have been studied in more detail to date, these materials often have magnetically ordered states that compete or coexist with the superconduct-

ing state, and such behavior tends to significantly complicate penetration depth measurements. For example, the heavy-fermion superconductor CePt$_3$Si first becomes magnetically ordered at 2.2 K before superconducting below 0.75 K,[3] and the two states have been shown to coexist on a microscopic level.[7] Transition-metal compounds such as Li$_2$$M_3$B ($M$ =Pd and Pt),[8,9] Mg$_{10}$Ir$_{19}$B$_{16}$,[10] and M_2Ga$_9$ (M=Rh and Ir) (Ref. 11) are therefore generally more straightforward systems for exploring the effect of SOC on superconductivity in the absence of inversion symmetry.

The strength of the SOC in any material is determined by both the crystallographic structure and the elemental composition. The latter is well illustrated through recent NMR (Ref. 12) and magnetic penetration depth[13] measurements on Li$_2$$M_3$B, which found that increasing SOC by replacing Pd with Pt changes the superconducting order parameter from dominantly spin singlet (Li$_2$Pd$_3$B) to nodal, spin triplet (Li$_2$Pt$_3$B). Muon spin rotation (μSR) measurements of the penetration depth in Li$_2$Pd$_3$B support the conclusion that Li$_2$Pd$_3$B is predominantly an s-wave BCS superconductor with only one isotropic energy gap.[14]

Mg$_{10}$Ir$_{19}$B$_{16}$ crystallizes in a noncentrosymmetric, body-centered cubic structure with space group $I\bar{4}3m$ and lattice constant a=10.568 Å.[15] A combination of resistivity, specific-heat, and magnetization measurements indicate that this material is a superconductor with T_c ranging between 4.5 and 5 K depending on the exact sample investigated.[10,16] Since Ir is a heavy transition-metal SOC is expected to be

strong in this material and so questions about the superconducting pairing symmetry are of significant interest.

The superconducting pairing symmetry of $Mg_{10}Ir_{19}B_{16}$ has already been investigated through both heat capacity[16,17] and photoemission spectroscopy,[18,19] and the data is consistent with isotropic *s*-wave pairing in both cases. However, point-contact spectroscopy[16] and penetration depth measurements performed using a tunnel diode oscillator[20] suggest that the system is better described by two-gap superconductivity. The two-gap model is consistent with spin-split bands that are a direct consequence of the lack of inversion symmetry combined with significant SOC, and is expected in the case of a mixed pairing state with a significant spin-triplet component. To help resolve the apparent disagreement regarding the nature of the superconducting pairing symmetry in $Mg_{10}Ir_{19}B_{16}$, more experiments need to be performed.

Muon spin rotation is a powerful technique for measuring the penetration depth and determining the nature of the pairing symmetry in superconductors. Due to maximal parity violation in the weak interaction decay of pions, the muons produced for such an experiment are initially ~100% spin polarized. Muon spin rotation employs a transverse-field geometry, as the muons are implanted into the sample one at a time with the initial polarization oriented perpendicular to the applied magnetic field. The muon spins exhibit Larmor precession about the local magnetic field and then decay into a positron, plus two neutrinos which are not detected. The resulting positron travels preferentially in the direction of the muon spin at the time of decay, and so due to the asymmetric nature of this decay one can track the polarization of the muon ensemble as a function of time by setting up positron counters around the sample. In type-II superconductors, the mixed (or vortex) state gives rise to a spatial distribution of local magnetic fields; this field distribution manifests itself in the μSR signal through a relaxation of the muon polarization. μSR has been used successfully for some time to study the mixed state in superconductors; further details can be found in Refs. 21 and 22.

Zero-field (ZF) μSR is very complementary to transverse field (TF) μSR superconductor studies. The experimental setup is essentially the same but no field is applied. μSR is an extremely sensitive probe of magnetism (internal fields on the order of 0.1 G can be readily detected), and so when investigating superconductors a ZF-μSR experiment is generally performed in advance of TF-μSR measurements to search for any anomalous magnetism that was not previously detected by other techniques. This knowledge is quite important since the presence of magnetism in a superconductor can significantly complicate penetration depth measurements.

ZF-μSR is also useful to search for time-reversal symmetry-breaking fields; the presence of such fields limits the possible superconducting states and the associated pairing symmetry. For example, time-reversal symmetry is a prerequisite for any spin-singlet state, but this symmetry is broken for certain spin-triplet states, specifically for those which have a degenerate representation. The presence of two or more degenerate superconducting phases naturally leads to a spatially inhomogeneous order parameter near the resulting domain walls; this creates spontaneous supercurrents and hence magnetic fields near those regions. Another possible
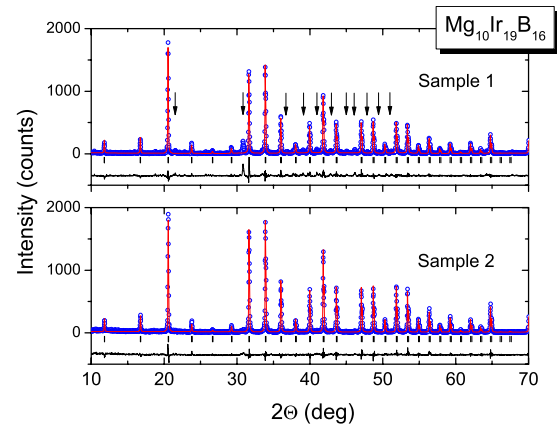

FIG. 1. (Color online) Powder x-ray diffraction measurements of the two $Mg_{10}Ir_{19}B_{16}$ samples used for the μSR measurements. The arrows indicate the dominant impurity peaks in the sample 1 pattern.

origin of time-reversal symmetry-breaking fields is from intrinsic magnetic moments due to spin polarization (for spin-triplet pairing) and the relative angular momentum of the Cooper pairs.[23] Broken time-reversal symmetry was previously detected in the unconventional superconductor Sr_2RuO_4 via μSR,[24] as a local field of ~0.5 G was found below T_c at the muon site. This provided some of the strongest evidence that Sr_2RuO_4 is actually a *p*-wave superconductor. Similar time-reversal symmetry-breaking fields could be detected by μSR if the spin-triplet contribution to the superconducting state in $Mg_{10}Ir_{19}B_{16}$ is significant.

In this work, we have used both ZF and TF-μSR to investigate the nature of the superconductivity in two polycrystalline $Mg_{10}Ir_{19}B_{16}$ samples of different quality. The former allowed us to search for time-reversal symmetry-breaking fields, and the latter allowed us to measure the penetration depth and characterize the pairing symmetry. Our data is consistent with single-gap, nodeless superconductivity; this is in agreement with the earlier heat capacity[17] and photoemission spectroscopy work.[18,19]

$Mg_{10}Ir_{19}B_{16}$ samples were synthesized by a standard solid-state reaction of pure Mg, Ir, and B elements as described elsewhere,[10] and the chemical composition was accurately determined via electron diffraction. Prior to the μSR measurements, the samples were characterized by powder x-ray diffraction, performed on a Scintag XDS 2000 diffractometer with Cu $K\alpha$ radiation (λ=0.15460 nm). Rietveld refinements of the structures were achieved using GSAS,[25,26] and slightly different lattice constants of 10.5629(4) Å and 10.5655(1) Å were found for sample 1 and 2, respectively. This is likely due to more vacancies in the crystal structure of the former, and when one also considers that many more impurity peaks are observed in the corresponding x-ray pattern (shown in Fig. 1), this suggests that sample 2 is a much higher quality specimen with fewer impurities/defects. The magnetic susceptibility of each sample was also measured with a superconducting quantum interference device magnetometer; the ZF-cooled (ZFC) and field-cooled (FC) measurements, shown in Fig. 2, confirmed nice superconducting properties. If we let T_c correspond to the onset of the suscep-
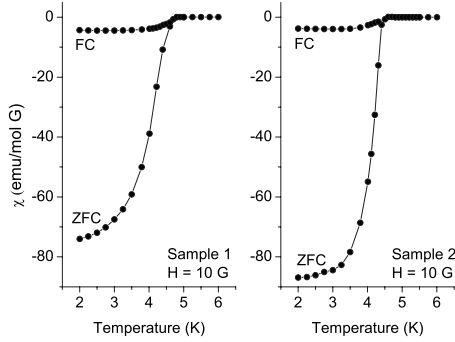
FIG. 2. ZFC and FC susceptibility measurements of the two $Mg_{10}Ir_{19}B_{16}$ samples used for the μSR measurements.

tibility drop, then $T_c \sim 4.8$ K for sample 1 and 4.6 K for sample 2. The much sharper drop below T_c, observed in both the FC and ZFC measurements of sample 2, provides further evidence for the better sample quality in this case.

ZF-μSR data was collected using the dilution refrigerator in conjunction with the M15 surface muon beamline at TRI-UMF. Figure 3 depicts normalized asymmetry vs time plots for both samples measured at temperatures of 0.1 and 6 K. This data was best fit to the form,

$$A(t) = A_0 e^{-\lambda t} G_{KT}(t), \qquad (1)$$

where $G_{KT}(t)$ is the Gaussian Kubo-Toyabe relaxation function given by

$$G_{KT}(t) = \frac{1}{3} + \frac{2}{3}(1 - \Delta^2 t^2)e^{-1/2\Delta^2 t^2}. \qquad (2)$$

The Gaussian Kubo-Toyabe relaxation is due to nuclear dipolar fields and is temperature independent; we determined this to be $\Delta = 0.207(4)$ μs^{-1} from a global fit incorporating all of our ZF data for the two samples. The exponential relaxation rate was set as a variable parameter and this is plotted as a function of temperature for the two samples in Fig. 4. Sample 1 shows a small increase in the exponential relax-
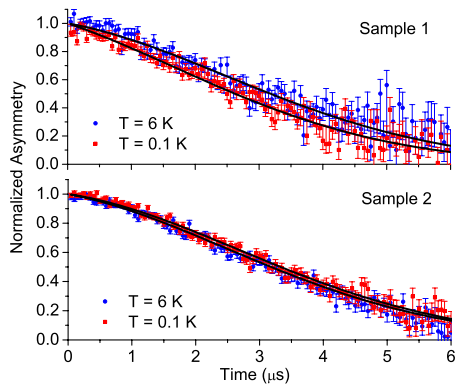

FIG. 3. (Color online) Normalized asymmetry vs time for the ZF-μSR measurements conducted on both samples at temperatures of 0.1 and 6 K. The fits, as described in the text, are superimposed on the data using solid black lines. A pronounced change is observed in the relaxation rate of sample 1 below T_c, but only a very small change is observed for sample 2.
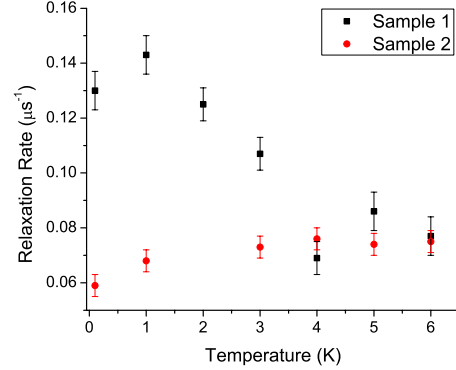

FIG. 4. (Color online) ZF-μSR relaxation rate vs temperature. The relaxation rate of sample 1 shows a small increase around T_c while the relaxation rate of sample 2 remains essentially constant within the error bars. Possible reasons for this discrepancy are outlined in the text.

ation rate of ~ 0.05 μs^{-1} below T_c, corresponding to a characteristic field strength of $B \sim 0.6$ G. However, the exponential relaxation rate of sample 2 remains essentially constant below T_c. Although we cannot completely rule out the presence of time-reversal symmetry-breaking fields in sample 2, the current data does set an upper bound on the magnitude of these fields to be ~ 0.05 G.

There are a few different scenarios that can explain the discrepancy between the ZF data of the two samples. One possibility is that the relaxation increase in sample 1 is actually due to time-reversal symmetry-breaking fields. The presence of such fields suggests that the associated superconducting state is at least twofold degenerate and the spatially varying order parameter would then lead to the presence of supercurrents in the bulk of the superconductor.[23] If this is the case, one would generally expect these fields to exist in sample 2 also, although we note that the domain size may be substantially smaller in sample 1 due to the poorer quality. Many more muons would then stop near the domain walls in sample 1 and see a nonzero local field associated with the currents flowing at the domain boundaries; this could lead to the increased broadening below T_c for this case only. Furthermore, NMR and electron-diffraction measurements were performed very recently on two similar samples with compositions $Mg_{9.3}Ir_{19}B_{16.7}$ and $Mg_{10.5}Ir_{19}B_{17.1}$.[27] The electron-diffraction measurements clearly confirmed that the former was a better quality sample with fewer defects/impurities and the NMR measurements indicated that only the other sample had a finite spin susceptibility in the zero-temperature limit. These results then suggested that defects/impurities may enhance spin-orbit coupling in this system thus leading to an increased spin-triplet component of the superconductivity; this interpretation is also consistent with the observation of time-reversal symmetry-breaking fields in our lower quality sample only.

There are also other possible explanations for the difference between the ZF data of the two samples not related to time-reversal symmetry-breaking fields. For example, the increased ZF relaxation in sample 1 could be due to dilute magnetic impurities throughout the sample. However, this seems rather unlikely since the onset of the increased relax-
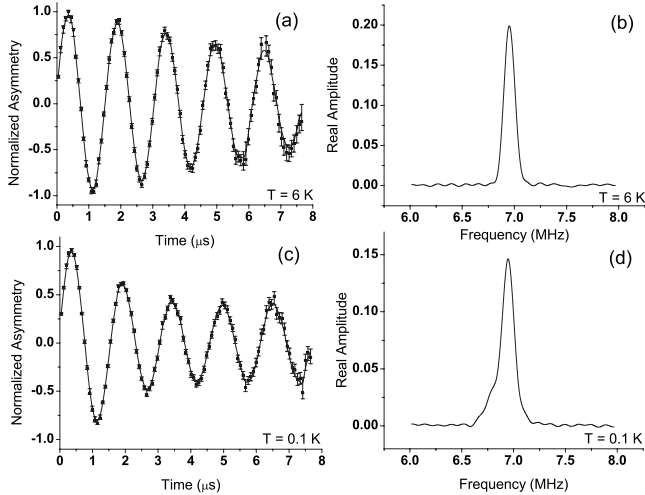
FIG. 5. $Mg_{10}Ir_{19}B_{16}$ sample 1 normalized asymmetry vs time and the corresponding fast-Fourier transforms at TF=500 G for both 6 K [shown in (a) and (b)] and 0.1 K [shown in (c) and (d)]. While the increased broadening is apparent for T=0.1 K, the characteristic Abrikosov line shape was not observed. This is likely due to the large background signal superimposed on the data.
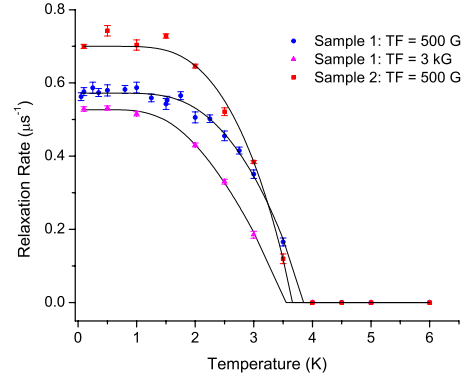

FIG. 6. (Color online) TF-μSR superconducting relaxation rate σ_{sc} vs temperature. The data can be adequately fit to a single-gap BCS model, as indicated by the solid lines.

$$A(t) = A_0 e^{-\sigma^2 t^2/2} \cos(\omega t + \phi) + A_{bg} \cos(\omega_{bg} t + \phi). \quad (3)$$

ation rate occurs very close to T_c and furthermore, these are not expected in this system. The other possibility is related to field zeroing. If the applied field was not perfectly zeroed in our experiment, there could potentially be some trapped flux in the superconducting state of these samples. Sample 1 may be more efficient at trapping flux than sample 2 due to the lower quality of the former and this could result in an increased relaxation below T_c for sample 1 only. We note that the ZF measurements were conducted on both samples back-to-back without ever applying a field during this time, and so any residual applied field should be the same for both samples.

While it is not possible for us to distinguish between these different scenarios, we can conclude with certainty that a high-purity sample of $Mg_{10}Ir_{19}B_{16}$ showed no evidence for time-reversal symmetry-breaking fields greater than 0.05 G. We also observed only very weak ZF relaxation in both samples at all temperatures, and so this allows for reliable penetration depth measurements to be performed.

With this in mind we proceeded to collect TF-μSR data, as measuring the penetration depth would allow us to learn more about the nature of the superconducting pairing symmetry. Note that all of the data was collected via field cooling. Figure 5 shows the fast-Fourier transforms obtained at both 6 and 0.1 K. Below T_c, the characteristic line shape of an Abrikosov vortex lattice was not resolved as a large background signal from the silver sample holder was superimposed on the data. However, we did find significant line broadening below T_c as expected for a superconductor (see Fig. 5). This broadening was analyzed as a Gaussian field distribution; the width of this distribution σ_{sc} has been shown previously to be proportional to the superfluid density $\sigma_{sc} \propto n_s / m^* \propto 1/\lambda^2$.[28] σ_{sc} was first obtained by fitting the μSR data in the time domain to the functional form,

The nonrelaxing background term was included to account for the muons stopping in the silver sample holder. The first term gives the total sample relaxation rate σ; there are contributions from both the vortex lattice and nuclear dipole moments below T_c. The contribution from the vortex lattice, σ_{sc}, was determined by quadratically subtracting the background nuclear dipolar relaxation rate obtained from spectra measured above T_c.

Figure 6 depicts the TF muon spin relaxation rate (proportional to superfluid density) vs temperature for our two $Mg_{10}Ir_{19}B_{16}$ samples. Sample 1 was investigated with both TF=500 G and 3 kG while sample 2 was investigated only in 500 G. The sample 1 data indicates that the superfluid density decreases with increasing applied field as expected. The superfluid density of the two samples at 500 G as $T \rightarrow 0$ is noticeably different; sample 2 has a higher superfluid density than sample 1 and this is consistent with the higher quality of the former. However, the temperature dependence of the superfluid density is the same for both samples: namely, the superfluid density seems to saturate as $T \rightarrow 0$. Since conventional BCS theory predicts an exponentially flat temperature dependence of the superfluid density at low temperatures, we proceeded to fit our data to this model. The agreement is quite good for both samples as seen in Fig. 6, and so this suggests that this material is characterized by a superconducting gap function with no nodes. For TF =500 G, fitting to the single-gap BCS model gave us the following parameters: $2\Delta/kT_c$=4.74(9) (2Δ=1.6 meV), T_c =3.8(1) K, and $\lambda(T \rightarrow 0)$=3570(20) Å for sample 1 and $2\Delta/kT_c$=4.93(5) (2Δ=1.6 meV), T_c=3.7(1) K and $\lambda(T \rightarrow 0)$=3230(20) Å for sample 2. Note that our $2\Delta/kT_c$ values are only slightly larger than what one expects for weak-coupled BCS theory and that the penetration depth values were obtained from σ_{sc} through a conversion procedure outlined in Ref. 29. The significantly suppressed T_c's in only a modest applied field of 500 G are consistent with the relatively low $H_{c2} \sim 8$ kG (Ref. 16) of this system.

Motivated by the earlier work proposing multigap superconductivity in $Mg_{10}Ir_{19}B_{16}$,[16,20] we also tried to fit our data to a phenomenological two-gap model as described

elsewhere.[30] Since the fitting routine assigned a weighting of 0 (within our error bars) to one of the gaps, we found that a two-gap model does not seem to describe our data unless the two gaps are very similar in magnitude. However, we note that previous measurements of $Mg_{10}Ir_{19}B_{16}$ suggesting multigap superconductivity were essentially performed in ZF while our μSR measurements were performed in an applied field. While a recent μSR penetration depth measurement performed by our group on the superconductor $Ba(Fe_{0.926}Co_{0.074})_2As_2$ found evidence for multigap superconductivity in that material, the same measurements also revealed that the relative weighting factor of the smaller gap quickly approaches 0 with increasing TF.[30] This could also be applicable to the present case.

Although the above results come with the warning that previous μSR measurements on polycrystalline cuprate samples have resulted in the correct temperature dependence of the superfluid density being masked, this may be less of a concern in the present case due to the cubic crystal symmetry and hence the isotropic penetration depth. In any event, future penetration depth measurements should be conducted on single crystals when they become available to confirm our results.

In conclusion, we have used both ZF and TF-μSR to investigate the superconductivity in two samples of the non-centrosymmetric system $Mg_{10}Ir_{19}B_{16}$. In the higher quality sample, ZF-μSR measurements find no evidence for time-reversal symmetry-breaking fields larger than 0.05 G. TF-μSR measurements of both samples yield a superfluid density that is exponentially flat at low temperatures, and so our data can be fit to a single-gap BCS model. These findings suggest that $Mg_{10}Ir_{19}B_{16}$ is a superconductor characterized by a single-gap function with no nodes. Our work also suggests that the superconducting properties of this system are very sensitive to sample quality and so further studies are required to investigate the roles of both SOC and defects/impurities on the superconductivity of this material in more detail.

[1] P. W. Anderson, J. Phys. Chem. Solids **11**, 26 (1959).

[2] P. W. Anderson, Phys. Rev. B **30**, 4000 (1984).

[3] E. Bauer, G. Hilscher, H. Michor, Ch. Paul, E. W. Scheidt, A. Gribanov, Yu. Seropegin, H. Noel, M. Sigrist, and P. Rogl, Phys. Rev. Lett. **92**, 027003 (2004).

[4] T. Akazawa, H. Hidaka, H. Kotegawa, T. C. Kobayashi, T. Fujiwara, E. Yamamoto, Y. Haga, R. Settai, and Y. Onuki, J. Phys. Soc. Jpn. **73**, 3129 (2004).

[5] N. Kimura, K. Ito, K. Saitoh, Y. Umeda, H. Aoki, and T. Terashima, Phys. Rev. Lett. **95**, 247004 (2005).

[6] I. Sugitani, Y. Okuda, H. Shishido, T. Yamada, A. Thamizhavel, E. Yamamoto, T. D. Matsuda, Y. Haga, T. Takeuchi, R. Settai, and Y. Onuki, J. Phys. Soc. Jpn. **75**, 043703 (2006).

[7] N. Metoki, K. Kaneko, T. D. Matsuda, A. Galatanu, T. Takeuchi, S. Hashimoto, T. Ueda, R. Settai, Y. Onuki, and N. Bernhoeft, J. Phys.: Condens. Matter **16**, L207 (2004).

[8] K. Togano, P. Badica, Y. Nakamori, S. Orimo, H. Takeya, and K. Hirata, Phys. Rev. Lett. **93**, 247004 (2004).

[9] P. Badica, T. Kondo, and K. Togano, J. Phys. Soc. Jpn. **74**, 1014 (2005).

[10] T. Klimczuk, Q. Xu, E. Morosan, J. D. Thompson, H. W. Zandbergen, and R. J. Cava, Phys. Rev. B **74**, 220502(R) (2006).

[11] T. Shibayama, M. Nohara, H. Aruga Katori, Y. Okamoto, Z. Hiroi, and H. Takagi, J. Phys. Soc. Jpn. **76**, 073708 (2007).

[12] M. Nishiyama, Y. Inada, and G.-Q. Zheng, Phys. Rev. Lett. **98**, 047002 (2007).

[13] H. Q. Yuan, D. F. Agterberg, N. Hayashi, P. Badica, D. Vandervelde, K. Togano, M. Sigrist, and M. B. Salamon, Phys. Rev. Lett. **97**, 017006 (2006).

[14] R. Khasanov, I. L. Landau, C. Baines, F. La Mattina, A. Maisuradze, K. Togano, and H. Keller, Phys. Rev. B **73**, 214528 (2006).

[15] Q. Xu, T. Klimczuk, T. Gortenmulder, J. Jansen, M. A. McGuire, R. J. Cava, and H. W. Zandbergen, Chem. Mater. **21**, 2499 (2009).

[16] T. Klimczuk, F. Ronning, V. Sidorov, R. J. Cava, and J. D. Thompson, Phys. Rev. Lett. **99**, 257004 (2007).

[17] G. Mu, Y. Wang, L. Shan, and H. H. Wen, Phys. Rev. B **76**, 064527 (2007).

[18] R. Yoshida, H. Okazaki, K. Iwai, K. Noami, T. Muro, M. Okawa, K. Ishizaka, S. Shin, Z. Li, J. Luo, G.-Q. Zheng, T. Oguchi, M. Hirai, Y. Muraoka, and T. Yokoya, J. Phys. Soc. Jpn. **78**, 034705 (2009).

[19] R. Yoshida, H. Okazaki, K. Iwai, K. Noami, T. Muro, M. Okawa, K. Ishizaka, S. Shin, Z. Li, J. Luo, G.-Q. Zheng, T. Oguchi, M. Hirai, Y. Muraoka, and T. Yokoya, Physica C **469**, 1034 (2009).

[20] I. Bonalde, R. L. Ribeiro, W. Bramer-Escamilla, G. Mu, and H. H. Wen, Phys. Rev. B **79**, 052506 (2009).

[21] J. E. Sonier, Rep. Prog. Phys. **70**, 1717 (2007).

[22] P. L. Russo, C. R. Wiebe, Y. J. Uemura, A. T. Savici, G. J. MacDougall, J. Rodriguez, G. M. Luke, N. Kaneko, H. Eisaki, M. Greven, O. P. Vajk, S. Ono, Y. Ando, K. Fujita, K. M. Kojima, and S. Uchida, Phys. Rev. B **75**, 054511 (2007).

[23] M. Sigrist and K. Ueda, Rev. Mod. Phys. **63**, 239 (1991).

[24] G. M. Luke, Y. Fudamoto, K. M. Kojima, M. I. Larkin, J. Merrin, B. Nachumi, Y. J. Uemura, Y. Maeno, Z. Q. Mao, Y. Mori, H. Nakamura, and M. Sigrist, Nature (London) **394**, 558 (1998).

[25] B. H. Toby, J. Appl. Crystallogr. **34**, 210 (2001).

[26] C. Larson and R. B. Von Dreele, Los Alamos National Laboratory Report No. LAUR 86, 2000 (unpublished).

[27] K. Tahara, Z. Li, H. X. Yang, J. L. Luo, S. Kawasaki, and G.-q. Zheng, Phys. Rev. B **80**, 060503(R) (2009).

[28] E. H. Brandt, Phys. Rev. B **37**, 2349 (1988).

[29] Y. J. Uemura, A. Keren, L. P. Le, G. M. Luke, B. J. Sternlieb, W.

D. Wu, J. H. Brewer, R. L. Whetten, S. M. Huang, S. Lin, R. B. Kaner, F. Diederich, S. Donovan, G. Gruner, and K. Holczer, Nature (London) **352**, 605 (1991).

30 T. J. Williams, A. A. Aczel, E. Baggio-Saitovitch, S. L. Bud'ko, P. C. Canfield, J. P. Carlo, T. Goko, J. Munevar, N. Ni, Y. J. Uemura, W. Yu, and G. M. Luke, Phys. Rev. B **80**, 094501 (2009).